

Magnetic susceptibility of semimagnetic semiconductors: The high-temperature regime and the role of superexchange

J. Spałek

*Department of Physics, Purdue University, West Lafayette, Indiana 47907
and Department of Solid State Physics, Akademia Gorniczo-Hutnicza (AGH), PL-30-059 Krakow, Poland**

A. Lewicki and Z. Tarnawski

Department of Solid State Physics, Akademia Gorniczo-Hutnicza (AGH), PL-30-059 Krakow, Poland

J. K. Furdyna

Department of Physics, Purdue University, West Lafayette, Indiana 47907

R. R. Galazka

Institute of Physics, Polish Academy of Sciences, PL-02-668 Warszawa, Poland

Z. Obuszko

Department of Solid State Physics, Akademia Gorniczo-Hutnicza (AGH), PL-30-059 Krakow, Poland

(Received 15 July 1985)

We present a systematic experimental study of the high-temperature susceptibility of diluted magnetic (semimagnetic) semiconductors $\text{Cd}_{1-x}\text{Mn}_x\text{Se}$, $\text{Cd}_{1-x}\text{Mn}_x\text{Te}$, and $\text{Hg}_{1-x}\text{Mn}_x\text{Se}$, and we analyze these together with the previously published results for $\text{Hg}_{1-x}\text{Mn}_x\text{Te}$ and $\text{Zn}_{1-x}\text{Mn}_x\text{Te}$. Despite their variety, all these materials reveal a common and very systematic pattern of behavior, which displays several interesting features. We formulate a theoretical model for the magnetic susceptibility in these systems in terms of the theory of a randomly dilute Heisenberg magnet, and we determine the dominant exchange integrals for each of the alloys by analyzing the available data according to this theory. The spin of Mn^{2+} ion in the first three compounds is also obtained and is found to be close to the atomic value of $S = \frac{5}{2}$. We find quantitative correlations between the exchange integrals for the three tellurides, and similarity for both selenides, and on the basis of these observations we argue that superexchange is the dominant mechanism determining the magnetic behavior of all those systems. Within this mechanism of exchange the p - d (anion- Mn^{2+}) and the d - d (Mn^{2+} - Mn^{2+}) exchange integrals can be related. Since in semimagnetic semiconductors both integrals can be obtained from independent measurements, these materials provide a unique opportunity for detailed experimental testing of superexchange.

I. INTRODUCTION

The purpose of this paper is threefold. First, we systematize the magnetic-susceptibility data for a series of diluted magnetic (semimagnetic) semiconductors in the high-temperature regime, within the framework of a theory which takes into account the effect of random dilution of magnetic ions in a nonmagnetic $A^{II}B^{VI}$ host semiconductor. Second, we determine the microscopic parameters (the exchange integral and the magnetic moment per magnetic ion) in these materials. Third, we show that the dominant interaction between the magnetic (Mn^{2+}) ions in both wide- and narrow-gap semiconductors takes place through the superexchange mechanism.

A characteristic feature¹ of this class of diluted magnetic semiconductors (DMS's) is the fact that they crystallize in the structure of the nonmagnetic $A^{II}B^{VI}$ semiconductor host (e.g., zinc blende for $\text{Cd}_{1-x}\text{Mn}_x\text{Te}$, $\text{Hg}_{1-x}\text{Mn}_x\text{Te}$, and $\text{Hg}_{1-x}\text{Mn}_x\text{Se}$, and wurtzite for $\text{Cd}_{1-x}\text{Mn}_x\text{Se}$). These structures differ from the corresponding Mn binary compounds MnSe and MnTe, which places an upper limit on

the value of x of the ternary alloys (for example, $x \leq 0.75$ for $\text{Cd}_{1-x}\text{Mn}_x\text{Te}$ and $x \leq 0.5$ for $\text{Cd}_{1-x}\text{Mn}_x\text{Se}$).

Although the magnetic properties of DMS's have received considerable attention during the last decade,²⁻⁴ no coherent microscopic interpretation of these properties has as yet emerged. While the complete picture of magnetic susceptibility in those materials still awaits formulation, we shall show that the behavior of magnetic susceptibility in the *high-temperature* limit is readily tractable in terms of a randomly dilute Heisenberg antiferromagnet. Our principal goal, then, is to present a complete set of high-temperature susceptibility data for $\text{Cd}_{1-x}\text{Mn}_x\text{Se}$, $\text{Cd}_{1-x}\text{Mn}_x\text{Te}$, and $\text{Hg}_{1-x}\text{Mn}_x\text{Se}$ in the full Mn concentration range available, to analyze them in terms of the above theory, and to extend the analysis to high-temperature data for other DMS's ($\text{Hg}_{1-x}\text{Mn}_x\text{Te}$, $\text{Zn}_{1-x}\text{Mn}_x\text{Te}$) available in the literature.^{5,6}

An added motivation for performing new magnetic measurements and a careful analysis of the data arises from the circumstance that considerable inconsistencies exist in much of the earlier susceptibility results. For ex-

ample, some workers have claimed that in these materials the Curie-Weiss temperature changes sign as a function of concentration,^{2,4} indicating a change from ferromagnetic to antiferromagnetic interaction between magnetic ions with increasing x . These and other anomalies (e.g., a concentration dependence of the effective spin per magnetic ion⁴) in the previously reported magnetic behavior of DMS's are eliminated by taking into account the diamagnetic contribution to the susceptibility, and by a systematic analysis of the data in the full concentration range within the framework of the theory developed below.

The understanding of magnetic susceptibility in DMS's is important not only because of its inherent interest as a problem in magnetism, but also because it bears on electrical and optical behavior of these systems, such as extremely large Faraday rotation,¹ giant negative magnetoresistance,⁷ the bound magnetic polaron,⁸ and other effects involving exchange interaction between the localized moments and band or impurity electrons.

The structure of the present paper is as follows. In Sec. II we give a short derivation of the equations for the susceptibility using the high-temperature expansion for a randomly dilute Heisenberg magnet. In Secs. III and IV we describe the experimental procedure and give a detailed analysis of the data on the basis of the theory developed in the preceding section. In Sec. V we determine the microscopic parameters: the value of the spin of Mn^{2+} ions and the dominant exchange integrals for $\text{Cd}_{1-x}\text{Mn}_x\text{Se}$, $\text{Cd}_{1-x}\text{Mn}_x\text{Te}$, and $\text{Hg}_{1-x}\text{Mn}_x\text{Se}$. We also compare these results with the exchange integrals for $\text{Hg}_{1-x}\text{Mn}_x\text{Te}$ and $\text{Zn}_{1-x}\text{Mn}_x\text{Te}$ obtained from the data already available in the literature.^{5,6} In Sec. VI we examine the values of the dominant exchange integrals for those systems, and we show that they are consistent with the predictions based on the superexchange mechanism. In that section we also relate the d - d and p - d exchange integrals, and we point out certain unique features afforded by DMS's for testing the superexchange process.

II. THEORETICAL DERIVATION OF THE HIGH-TEMPERATURE SUSCEPTIBILITY

In this section we derive the Curie-Weiss law from the high-temperature expansion of the static magnetic susceptibility. This will give the dependence on the Mn concentration of such parameters as the Curie constant and the Curie-Weiss temperature, as well as the relationship of these macroscopic parameters with the effective magnetic moment and the exchange integrals.

We assume that Mn^{2+} ions in DMS's are orbitally nondegenerate (i.e., in the $L=0$ state), and hence we can represent the interactions between them through the Heisenberg Hamiltonian for a randomly dilute antiferromagnet:

$$H = \sum_{i,j'} J_{ij} \mathbf{S}_i \cdot \mathbf{S}_j \xi_i \xi_j - g\mu_B \mathbf{H}_a \cdot \sum_i \mathbf{S}_i \xi_i, \quad (2.1)$$

where sums over i and j run over all lattice sites ($i \neq j$), and ξ_i is 0 or 1 depending on whether the cation site is occupied by a nonmagnetic (Cd^{2+} , Hg^{2+} , or Zn^{2+}) or a magnetic (Mn^{2+}) ion, respectively. J_{ij} is the exchange in-

tegral, and \mathbf{S}_i is the atomic spin of the magnetic ion located on the i th site. The last term in Eq. (2.1) is the Zeeman term, with \mathbf{H}_a denoting the applied field. A given sequence $\{\xi_i\}$ of two-valued operators $\xi_i=0,1$ determines a specific distribution of magnetic and nonmagnetic atoms on the lattice sites. Hence, we have to average the results derived for the Hamiltonian (2.1) for a given distribution $\{\xi_i\}$ with respect to all equivalent configurations of the two sets of cations. For a substitutionally disordered mixture of nonmagnetic and magnetic cations, such an averaging procedure yields $\bar{\xi}_i = \bar{\xi}_i^2 = x$.

The static longitudinal susceptibility per unit volume is defined by

$$\chi = -\frac{1}{V} \left[\frac{\partial^2 F}{\partial H_a^2} \right]_T, \quad (2.2)$$

where V is the volume of the system, and F is its free energy, given by

$$F = -k_B T \sum_{\xi_1, \xi_2, \dots, \xi_N} P(\xi_1, \xi_2, \dots, \xi_N) \ln \text{Tr} e^{-\beta H} \\ \equiv -k_B T \overline{\ln Z}. \quad (2.3)$$

In this expression $P(\xi_1, \xi_2, \dots, \xi_N)$ is the probability distribution of having a given sequence $(\xi_1, \xi_2, \dots, \xi_N)$, Tr denotes the trace over all spin degrees of freedom, Z is the partition function for a particular configuration $\{\xi_i\}$, and $\beta \equiv (k_B T)^{-1}$ is the inverse temperature in energy units. Substituting Eq. (2.1) into (2.3) and performing the derivatives in Eq. (2.2), one obtains the expression for χ of a paramagnetic system and for $H_a=0$,

$$\chi = \frac{(g\mu_B)^2}{k_B T V} \sum_{i,j} \overline{\langle \xi_i \xi_j S_i^z S_j^z \rangle_{T, H_a=0}}, \quad (2.4)$$

where g is the Landé factor and μ_B is the Bohr magneton. This is our starting equation, in which $\langle \dots \rangle$ denotes the quantum average for a given sequence $\{\xi_i\}$, S_i^z is the z component of the spin \mathbf{S}_i , and $\overline{\langle \dots \rangle}$ denotes a configuration average.

Expression (2.4) is exact, but difficult to analyze in general. In order to perform explicit calculations, we therefore resort to the high-temperature expansion. That is to say, we write the relevant correlation function as

$$\langle \xi_i \xi_j S_i^z S_j^z \rangle = \xi_i \xi_j \frac{\text{Tr}(S_i^z S_j^z e^{-\beta H})}{\text{Tr}(e^{-\beta H})} \equiv \xi_i \xi_j \langle S_i^z S_j^z \rangle, \quad (2.5)$$

and subsequently make the following expansion:

$$\langle S_i^z S_j^z \rangle = \frac{\text{Tr}[S_i^z S_j^z (1 - \beta H + \frac{1}{2} \beta^2 H^2 + \dots)]}{\text{Tr}(1 - \beta H + \frac{1}{2} \beta^2 H^2 + \dots)}. \quad (2.6)$$

Noting that $\text{Tr} H = 0$, we then have, to first order in βH ,

$$\langle S_i^z S_j^z \rangle \simeq \frac{\text{Tr}(S_i^z S_j^z)}{\text{Tr} 1} - \beta \frac{\text{Tr}(S_i^z S_j^z H)}{\text{Tr} 1} \\ \equiv \langle S_i^z S_j^z \rangle_\infty - \beta \langle S_i^z S_j^z H \rangle_\infty, \quad (2.7)$$

where $\langle \dots \rangle_\infty$ means the statistical average taken at infinite temperature. The advantage of expressing $\langle S_i^Z S_j^Z \rangle$ through the averages $\langle \dots \rangle_\infty$ is that then the coefficients of the expansion (2.7) can be calculated directly, since at $T = \infty$ spins on different sites can be regarded as completely independent. Starting with this notion, one can evaluate the traces⁹ and get

$$\langle S_i^Z S_j^Z \rangle_\infty = \delta_{ij} \langle (S_i^Z)^2 \rangle_\infty = \frac{1}{3} S(S+1) \delta_{ij}, \quad (2.8)$$

$$\begin{aligned} \langle S_i^Z S_j^Z H \rangle_\infty &= \sum_{kl'} \sum_{\alpha=1}^3 J_{kl} \xi_k \xi_l \langle S_i^Z S_j^Z S_k^\alpha S_l^\alpha \rangle_\infty \\ &= \frac{2}{9} [S(S+1)]^2 J_{ij} \xi_i \xi_j, \end{aligned} \quad (2.9)$$

where S is the magnitude of the atomic spin ($S = \frac{5}{2}$ for the atomic $3d^5$ state of Mn^{2+}). Substituting Eqs. (2.8) and (2.9) in Eq. (2.7), we finally obtain an expression for χ ,

$$\chi = \frac{(g\mu_B)^2 S(S+1)x}{3k_B T} \frac{N}{V} \left[1 - \frac{2[S(S+1)]^2}{3k_B T} \frac{\sum_{i,j} J_{ij} \xi_i \xi_j}{NxS(S+1)} \right], \quad (2.10)$$

where x is the atomic fraction of magnetic ions, and N is the total number of cation sites in volume V . Furthermore, for a random arrangement of magnetic ions

$$\overline{\xi_i \xi_j} = \begin{cases} \xi_i^2 = \xi_j^2 = x & \text{for } i=j, \\ \xi_i \xi_j = x^2 & \text{for } i \neq j. \end{cases} \quad (2.11)$$

Making use of this fact and noting that, to first order in $A/k_B T$,

$$1 - \frac{A}{k_B T} = \left[1 + \frac{A}{k_B T} \right]^{-1},$$

we recast Eq. (2.10) in the form of the Curie-Weiss law

$$\chi = \frac{C(x)}{T - \Theta(x)}, \quad (2.12)$$

with the Curie constant per unit volume

$$C(x) = x \frac{(g\mu_B)^2 S(S+1)}{3k_B} \frac{N}{V} \equiv C_0 x, \quad (2.13)$$

and the Curie-Weiss temperature

$$\Theta(x) = -\frac{2}{3} x S(S+1) \sum_P J_{PzP} / k_B \equiv \Theta_0 x. \quad (2.14)$$

In this expression J_P is the exchange integral for a pair of P th neighbors, and z_P is the number of cations on the P th coordination sphere around a given cation chosen as the central one, since we have replaced the sum $\sum_{i,j} J_{ij}$ by $N \sum_P J_{PzP}$.

One sees that, if the distribution of magnetic atoms on the lattice is truly random, then both the Curie constant and the Curie-Weiss temperature scale linearly with x . The values C_0 and Θ_0 correspond to the limiting values of

$C(x)$ and $\Theta(x)$ for a hypothetical magnetic semiconductor with $x=1$, and with the crystallographic structure of the host semiconductor $A^{II}B^{VI}$ (i.e., MnSe and MnTe in the wurtzite or zinc-blende structures). The susceptibility χ itself does not scale linearly with x , but according to

$$\chi = \frac{C_0 x}{T - \Theta_0 x}. \quad (2.15)$$

We note parenthetically that Eq. (2.12) was derived in the asymptotic regime $T \gg |\Theta(x)|$. Extending the analysis to one order higher in $1/T$, one can show that it leads to the replacement of Eq. (2.12) by

$$\chi^{-1} = \frac{1}{C(x)} \left[T - \Theta(x) + \frac{1}{T} [\Theta(x)^2 - A(x)] \right], \quad (2.16)$$

where

$$A(x) = [\Theta(x)]^2 + \frac{8}{9} [S(S+1)]^2 \sum_P J_{PzP}^2 x^2. \quad (2.17)$$

In the special case of one (nearest-neighbor) exchange integral, this equation reduces to

$$A(x) = [\Theta(x)]^2 \frac{z+2}{z}, \quad (2.18)$$

where z is the number of nearest neighbors. It is then evident that $[\Theta(x)]^2 < A(x)$, and hence the higher-order correction is negative. This means that the inverse susceptibility will bend downward with decreasing temperature, as is observed experimentally in all cases studied by us, as well as in Refs. 2 and 6.

Finally, we would like to comment on the units chosen. The value $C(x)$ given by Eq. (2.13) is per unit volume. Since the lattice parameter varies (linearly) with x , hence N/V will depend on x . To avoid this x dependence, we find it convenient to introduce in place of $C(x)$ the molar Curie constant $C_M(x)$, related to $C(x)$ through

$$C_M(x) = \frac{C(x)}{\rho(x)} \mu(x),$$

where $\rho(x)$ is the density for a given x , and $\mu(x)$ is the corresponding molar mass for the given $A_{1-x}^{II} \text{Mn}_x B^{VI}$ alloy, e.g.,

$$\mu(x) = (1-x)\mu_{\text{CdTe}} + x\mu_{\text{MnTe}}.$$

As in the case of $C(x)$, for the molar Curie constant we have

$$C_M(x) = C_M x,$$

where C_M corresponds to $C_M(x=1)$.

III. EXPERIMENT

The static susceptibility measurements were carried out using the Faraday method, with force compensation¹⁰ of the order of 10^{-7} N. The system was calibrated using a standard Er_2O_3 sample with a known value of χ . The measurements of magnetization $M(T, H_a)$ were performed in two stages. First, we measured the field dependence of magnetization $M(H_a)$ for a given temperature. The function $M(H_a)$ was linear in the field range up to

10 kOe and for $T \geq 77$ K. The susceptibility χ was then obtained directly from the relation $M = \chi H_a$. The diamagnetic contributions for CdSe, CdTe, and HgSe ($\chi_d = -0.334 \times 10^{-6}$, -0.345×10^{-6} , and -0.30×10^{-6} emu/g, respectively¹¹) were then subtracted from the data for χ . The maximal error estimated was 0.03×10^{-6} mu/g. One can therefore take χ_d as $-(0.33 \pm 0.03) \times 10^{-6}$ emu/g in all cases reported.

Second, we repeated the whole procedure for various temperatures up to room temperature. The temperature dependence of inverse susceptibility $\chi^{-1}(T)$ for a given concentration x of Mn was fitted to the Curie-Weiss law by the weighted least-squares method. The method of fitting was chosen to give the condition $\Theta(x=0)=0$ and $C_M(x=0)=0$ within the fitting accuracy, since in the absence of magnetic ions the susceptibility should correspond to that of an ordinary (i.e., nonmagnetic) semiconductor.

The concentration regimes studied were $0.01 \leq x \leq 0.45$ for $\text{Cd}_{1-x}\text{Mn}_x\text{Se}$, $0 < x \leq 0.70$ for $\text{Cd}_{1-x}\text{Mn}_x\text{Te}$, and $0.057 \leq x \leq 0.18$ for $\text{Hg}_{1-x}\text{Mn}_x\text{Se}$. The samples were monocrystalline, prepared by the vertical Bridgman method described elsewhere.¹² The results for crystals $\text{Zn}_{1-x}\text{Mn}_x\text{Te}$ and $\text{Hg}_{1-x}\text{Mn}_x\text{Te}$, used for comparison with the present data, were also described previously.^{5,6} It is our experience (based on measurements on scores of samples) that in the case of the Cd-based alloys the actual Mn concentration is usually within $\pm 5\%$ of the nominal concentration. For example, a $\text{Cd}_{1-x}\text{Mn}_x\text{Te}$ sample with nominal $x=0.10$ can be expected to have x between 0.095 and 0.105. Thus, in the case of $\text{Cd}_{1-x}\text{Mn}_x\text{Se}$ and $\text{Cd}_{1-x}\text{Mn}_x\text{Te}$ we used nominal concentrations in our analysis. The situation is different in the case of Zn-based or Hg-based alloys, which display serious concentration gradients in the process of Bridgman growth. In the case of those alloys we therefore used the concentrations deter-

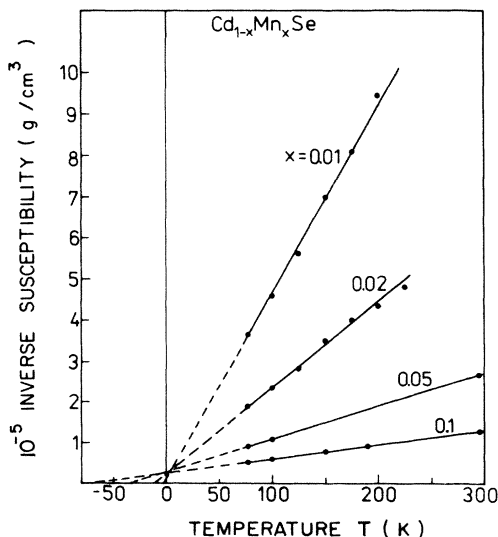


FIG. 1. Inverse magnetic susceptibility per unit mass for $\text{Cd}_{1-x}\text{Mn}_x\text{Se}$ as a function of temperature, for various concentrations $0 < x \leq 0.1$.

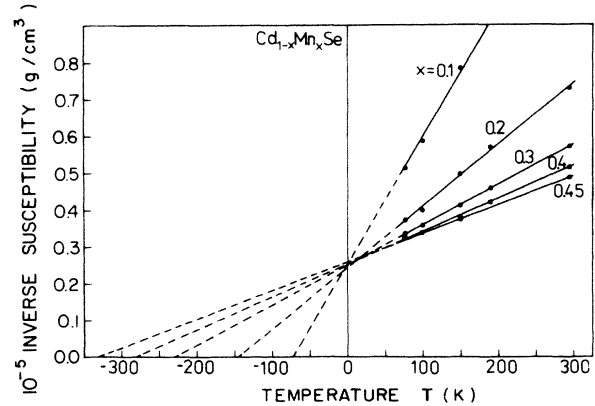


FIG. 2. Same as Fig. 1, but for $0.1 \leq x \leq 0.45$. Note that all curves here and on the preceding figure have a common intercept on the y axis. The extrapolation of the curves to the negative temperature axis gives the Curie-Weiss temperature $\Theta(x)$.

mined by electron microprobe analysis or chemical wet analysis obtained on specimens adjacent to the samples used in the susceptibility measurements.

IV. EXPERIMENTAL RESULTS

A. $\text{Cd}_{1-x}\text{Mn}_x\text{Se}$ and $\text{Cd}_{1-x}\text{Mn}_x\text{Te}$

The results concerning the inverse susceptibility in the high-temperature regime for $\text{Cd}_{1-x}\text{Mn}_x\text{Se}$ are given in Figs. 1 and 2, and those for $\text{Cd}_{1-x}\text{Mn}_x\text{Te}$ are shown in Figs. 3 and 4. The fit to the Curie-Weiss law is good in the full range of Mn concentrations available.¹³ In particular, the straight lines in the figures verify the interesting prediction of the theory that at $T=0$ the intercept of the extrapolated high-temperature values of χ^{-1} is independent of x [cf. Eq. (2.15)].

The values of the effective Curie-Weiss temperature $\Theta(x)$ and the molar Curie constant $C_M(x)$ were fitted to

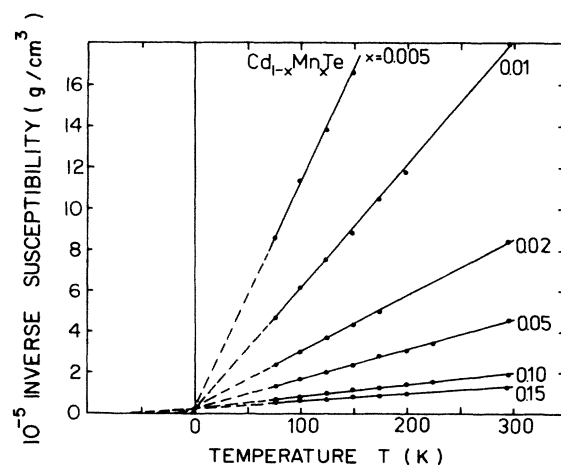


FIG. 3. Same as Fig. 1, but for $\text{Cd}_{1-x}\text{Mn}_x\text{Te}$ and for $0.005 < x \leq 0.15$.

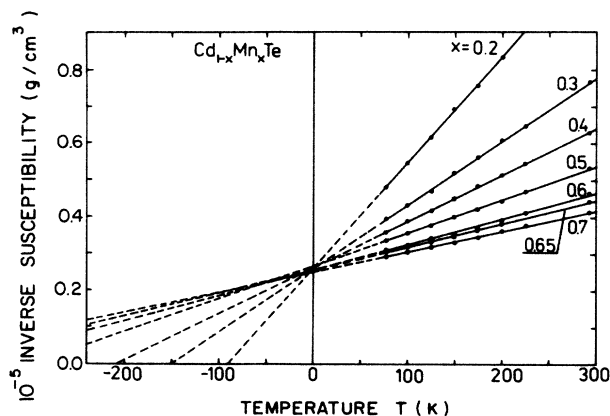


FIG. 4. Same as Fig. 1, but for $\text{Cd}_{1-x}\text{Mn}_x\text{Te}$ and for $0.2 \leq x \leq 0.7$. The extrapolation of the curves to the negative temperature axis gives the Curie-Weiss temperature $\Theta(x)$.

the straight lines $ax + b$. The value of b was in each case equal to zero within the fitting accuracy. The data concerning $\Theta(x)$ and $C_M(x)$ are shown in Figs. 5 and 6 for $\text{Cd}_{1-x}\text{Mn}_x\text{Se}$ and in Figs. 7 and 8 for $\text{Cd}_{1-x}\text{Mn}_x\text{Te}$, respectively. From these data the values of Θ_0 and C_M were determined from the slope of $\Theta(x)$ and $C_M(x)$, respectively, and are given in Table I.

One notices in Figs. 7 and 8 that at the highest concentrations the results for $\text{Cd}_{1-x}\text{Mn}_x\text{Te}$ deviate appreciably from the corresponding straight lines. In Sec. VI we propose a natural explanation of this behavior. However, an upward bending of $C_M(x)$ for $x \geq 0.4$, as shown in Fig. 8, is inconsistent with the strict requirements of the present model, in which the Curie constant should be proportional to the number of magnetic ions in the system.¹³

A possible explanation of the deviation of $C_M(x)$ from the straight line in Fig. 8 may be as follows. For $x \approx 0.65$

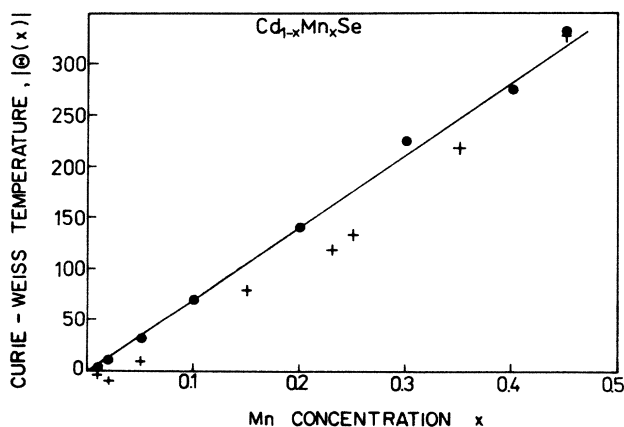


FIG. 5. Magnitude of the Curie-Weiss temperature $\Theta(x)$ (which itself is negative) for $\text{Cd}_{1-x}\text{Mn}_x\text{Se}$ as a function of x . The crosses (+) are taken from Ref. 4 and are drawn for comparison.

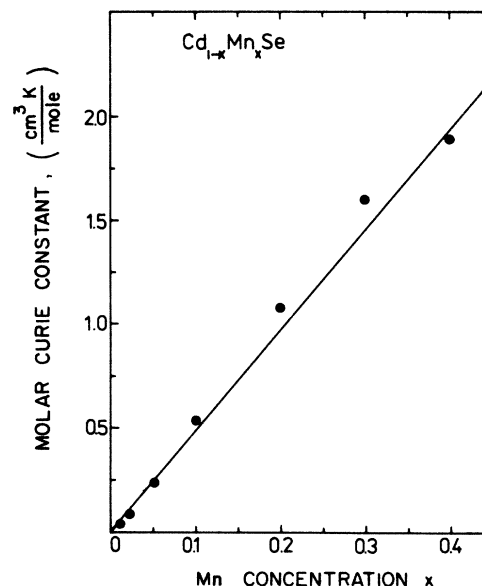


FIG. 6. Molar Curie constant $C_M(x)$ for $\text{Cd}_{1-x}\text{Mn}_x\text{Se}$ as a function of x . The solid line is the fitted straight line which gives $C_M(x=0)=0$ within the fitting accuracy.

the value of $\Theta(x) \approx -300$ K, comparable in magnitude to the maximal temperature at which the measurements were done. Strictly speaking, representation of the data via the Curie-Weiss law should be valid only when $|\Theta(x)|$ is substantially smaller than the measurement temperature T . The observed deviation of $C_M(x)$ from the linear behavior $C_M(x) = C_M x$ may thus be due to the fact that for $x > 0.4$ the value of $|\Theta(x)| \gtrsim 200$ K, too large to satisfy the expansion conditions on which the present analysis (Sec. II) is based. In the following discussion we therefore determine the microscopic parameters (such as the effective spin per Mn^{2+} ion and the dominant exchange integral) using the data from the region of concentrations where $\Theta(x)$ and $C_M(x)$ scale linearly with x .

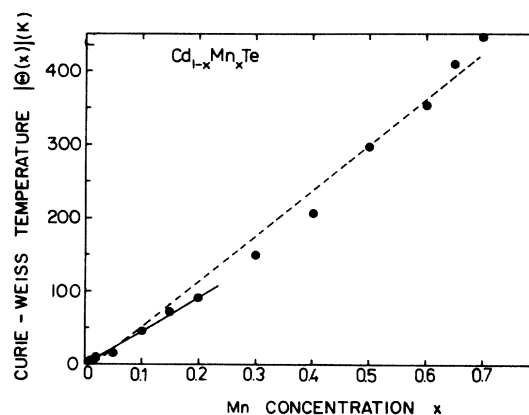


FIG. 7. Same as Fig. 3, but for $\text{Cd}_{1-x}\text{Mn}_x\text{Te}$. The solid line is the fitted line which gives a good representation of the data for $x \leq 0.2$. The dashed line shows that fitting of the data to a straight line in the whole range of $x \leq 0.7$ leads to an unphysical result where the fitted line does not pass through the origin (for an explanation, see the text).

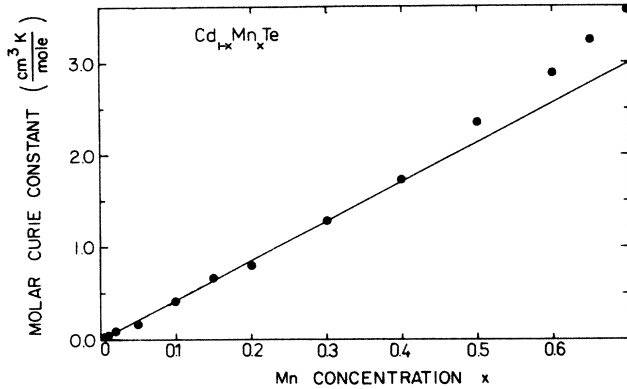


FIG. 8. Same as Fig. 6, but for $\text{Cd}_{1-x}\text{Mn}_x\text{Te}$. The fit is good only for $x \lesssim 0.4$.

B. $\text{Hg}_{1-x}\text{Mn}_x\text{Se}$ and $\text{Hg}_{1-x}\text{Mn}_x\text{Te}$

Since we are going to compare wide- and narrow-gap semiconductors from the point of view of the nature of exchange interactions involved in those systems, we have reexamined the high-temperature data for $\text{Hg}_{1-x}\text{Mn}_x\text{Se}$ and $\text{Hg}_{1-x}\text{Mn}_x\text{Te}$ as well. Figures 9 and 10 represent the concentration dependences of $\Theta(x)$ and $C_M(x)$ for $\text{Hg}_{1-x}\text{Mn}_x\text{Se}$, together with the theoretical straight lines. From those figures we have again determined the values of Θ_0 and C_M given in Table I. On the other hand, the value of $\Theta_0 = (-500 \pm 10)$ K for $\text{Hg}_{1-x}\text{Mn}_x\text{Te}$ is taken from the data of Nagata *et al.*⁵

C. $\text{Zn}_{1-x}\text{Mn}_x\text{Te}$

We have also reexamined the data of McAlister *et al.*⁶ concerning the concentration dependence of the Curie-Weiss temperature for $\text{Zn}_{1-x}\text{Mn}_x\text{Te}$. The data of $\Theta(x)$ versus x is shown in Fig. 11, the solid line being a straight-line fit $\Theta(x) = \Theta_0 x$. The slight curvature downward of $\Theta(x)$ for higher concentrations⁶ (not marked in Fig. 11) is similar to that shown in Fig. 7 for

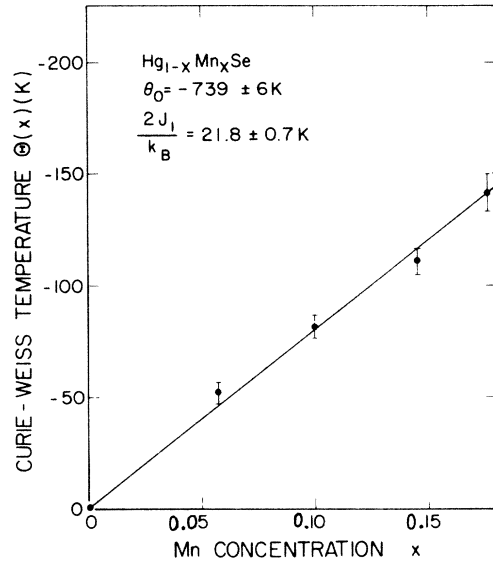


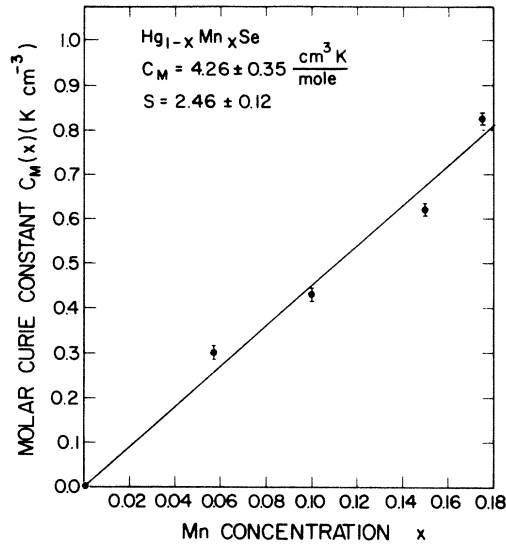
FIG. 9. Same as Fig. 5, but for $\text{Hg}_{1-x}\text{Mn}_x\text{Se}$.

$\text{Cd}_{1-x}\text{Mn}_x\text{Te}$, and will be dealt with in Sec. VI.

Summarizing this section, one can say that our data for all DMS's with Mn^{2+} ions can be represented by the Curie-Weiss law. In the regime of concentration in which $\Theta(x)$ is substantially smaller than the temperature range over which the measurements were performed, the concentration dependence of $\Theta(x)$ and $C_M(x)$ is linear, in agreement with the prediction of the theory which assumes a completely random distribution of Mn atoms on cation sites. We have also studied the deviation from the straight line $\Delta\Theta \equiv \Theta(x) - \Theta_0 x$ as a function of x for $\text{Cd}_{1-x}\text{Mn}_x\text{Te}$. The deviation can be represented by the function $\Delta\Theta \equiv 371x^3$, as shown in Fig. 12. This particular behavior is discussed in Sec. VI, where we introduce the concept of superexchange in a tetrahedral configuration of cations surrounding a distorted anion position. The value of $\Theta(x)$ is negative for all concentrations of Mn, contrary to what has been claimed by some earlier investigators for low concentrations, $x \leq 0.05$ (cf. Refs. 2 and 4). The opposite sign of Θ for low Mn concentrations would indeed arise when the diamagnetic contribution due to the filled shells of the host semiconductor is not taken into account. This is very likely the reason why these authors^{2,4} observed a change of sign of Θ for $x < 0.05$.

TABLE I. Values of parameters determined from susceptibility data.

Material	Θ_0 (K)	C_M $\left[\frac{\text{cm}^3 \text{K}}{\text{mole}} \right]$	Spin S	$2J_1/k_B$ (K)	Crystal structure
$\text{Cd}_{1-x}\text{Mn}_x\text{Se}$	-743 ± 15	4.81 ± 0.1	2.64 ± 0.06	21.2 ± 0.4	wurtzite
$\text{Cd}_{1-x}\text{Mn}_x\text{Te}$	-470 ± 34	4.27 ± 0.17	2.47 ± 0.05	13.8 ± 0.3	zinc blende
$\text{Hg}_{1-x}\text{Mn}_x\text{Se}$	-739 ± 47	4.26 ± 0.35	2.46 ± 0.12	21.8 ± 1.4	zinc blende
$\text{Hg}_{1-x}\text{Mn}_x\text{Te}$	-500 ± 10			14.3 ± 0.5	zinc blende
$\text{Zn}_{1-x}\text{Mn}_x\text{Te}$	-831 ± 63			23.7 ± 0.5	zinc blende

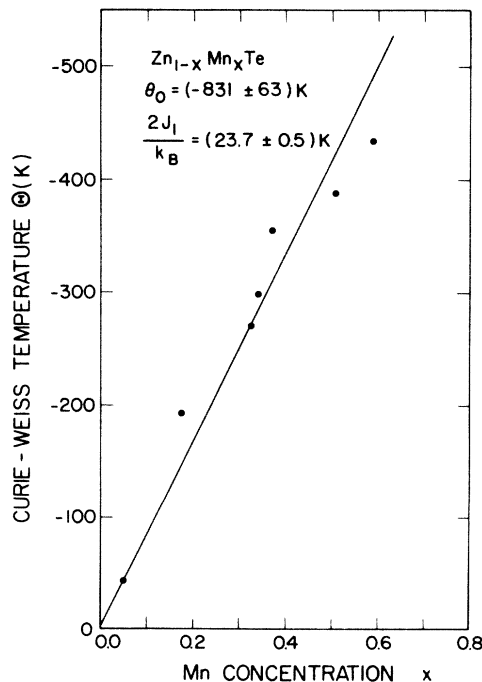
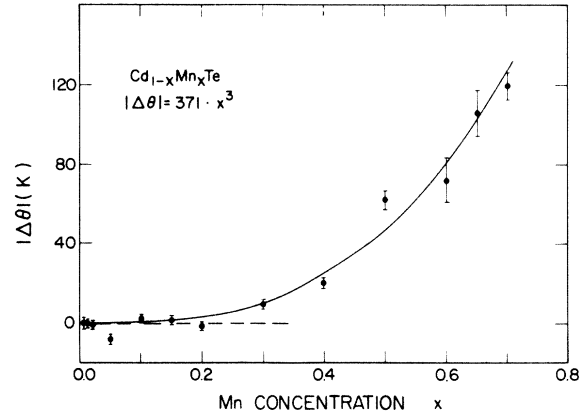
FIG. 10. Same as Fig. 6, but for $\text{Hg}_{1-x}\text{Mn}_x\text{Se}$.

V. MICROSCOPIC PARAMETERS S AND J

From the values of the molar Curie constant C_M one can determine the effective spins per Mn^{2+} ion, since

$$S(S+1) = \frac{3C_M k_B}{(g\mu_B)^2 N_{\text{Avogadro}}}, \quad (5.1)$$

where N_{Avogadro} is the Avogadro number. We assume that Mn^{2+} ions are in $L=0$ state, and therefore one can

FIG. 11. Same as Fig. 5, but for $\text{Zn}_{1-x}\text{Mn}_x\text{Te}$ (after Ref. 6).FIG. 12. Deviation $|\Delta\Theta|$ of the actual Curie-Weiss temperature $\Theta(x)$ of $\text{Cd}_{1-x}\text{Mn}_x\text{Te}$ from the value Θ_0x obtained from the Curie-Weiss law, as a function of x . The fitted curve is $|\Delta\Theta| = 371x^3$.

assume $g=2$. This assumption is fully supported by EPR measurements.¹⁴ One then obtains $S = 2.62 \pm 0.06$, 2.47 ± 0.05 , and 2.54 ± 0.05 , for $\text{Cd}_{1-x}\text{Mn}_x\text{Se}$, $\text{Cd}_{1-x}\text{Mn}_x\text{Te}$, and $\text{Hg}_{1-x}\text{Mn}_x\text{Se}$, respectively. Only the first value is about 3% larger than the atomic value $S = \frac{5}{2}$ for the $3d^5$ configuration of d electrons with Hund's rule fulfilled. Thus, to a good approximation one can take $S = \frac{5}{2}$ as the value of S in the regime where $C_M(x)$ varies linearly with x . Oseroff⁴ calculated the value of S for each concentration x separately and found it growing with x . We do not observe such a dependence when we limit our analysis to the concentration $x \leq 0.2$, where the Curie-Weiss law is applicable (cf. the discussion in Sec. III A).

From the values of Θ_0 listed in Table I one can estimate the dominant exchange integral J_1 between the nearest neighbors,

$$\frac{2J_1}{k_B} = \frac{3\Theta_0}{zS(S+1)}. \quad (5.2)$$

The factor "2" in Eq. (5.2) arises from the fact that, when summing over all possible pairs $\langle ij \rangle$ in the exchange part of Eq. (2.1), we count each pair twice. Taking the number of nearest neighbors $z=12$ for both wurtzite and zincblende structures, we get the values of $2J_1/k_B$ listed in Table I. These values will be correlated with the cation-cation distance and with the type of anion in the next section.

We should remark here that the value of J_1 given by Eq. (5.2) neglects the effect of the exchange integral between the next-nearest neighbors. Recall that, in general, $\Theta \sim J_1z + J_2z_2$ [cf. Eq. (2.14)]. Hence, the value J_1 determined here is, strictly speaking, equal to

$$J_1(1 + J_2z_2/J_1z).$$

Since for a half-filled d shell we expect that the superexchange integrals are antiferromagnetic, our value of J_1 in Table I is then expected to be an upper estimate.

VI. DISCUSSION AND INTERPRETATION OF RESULTS

A. Comparative analysis of DMS's and the role of superexchange

In this section we would like to systematize the results presented above, and to show that the exchange integrals of the various systems can be correlated when the superexchange mechanism is invoked. In order to compare the exchange integrals, we use the data on cation-cation distance in DMS's provided by Yoder-Short *et al.*,¹⁵ which are plotted in Fig. 13. The convenience of this plot arises from the fact that the tetrahedral configuration of nearest cations surrounding an anion is the same for both wurtzite and zinc-blende materials. Thus, from the point of view of nearest-neighbor cation (or anion) distances, these two classes of materials can be discussed together.

From Fig. 13 we see that for the pairs ($\text{Cd}_{1-x}\text{Mn}_x\text{Te}$, $\text{Hg}_{1-x}\text{Mn}_x\text{Te}$) and ($\text{Cd}_{1-x}\text{Mn}_x\text{Se}$, $\text{Hg}_{1-x}\text{Mn}_x\text{Se}$) this distance is quite close. We observe that the corresponding exchange integrals J_1 from Table I are also close within each pair, i.e., we obtain the values ($2J_1/k_B = 13.8 \pm 0.3$ and 14.3 ± 0.5 K) for the pair ($\text{Cd}_{1-x}\text{Mn}_x\text{Te}$, $\text{Hg}_{1-x}\text{Mn}_x\text{Te}$), and (21.2 ± 0.4 and 21.8 ± 0.5 K) for ($\text{Cd}_{1-x}\text{Mn}_x\text{Se}$, $\text{Hg}_{1-x}\text{Mn}_x\text{Se}$), respectively. Note that in the case of each pair the alloys yield close values of the exchange integral, irrespective of the fact that the band gap is strikingly different for the two members of each pair, particularly at low x . Hence, one

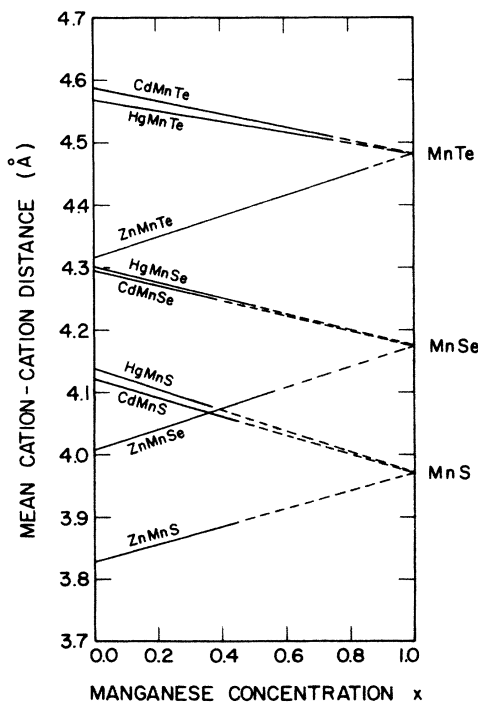


FIG. 13. Cation-cation distance for various DMS's. The extreme points on the right labeled MnTe, MnSe, and MnS correspond to the cation-cation distances in the hypothetical tetrahedrally bonded magnetic semiconductors MnX ($X = \text{S}, \text{Se}, \text{or Te}$) (after Ref. 15).

is forced to conclude that the Bloembergen-Rowland mechanism of exchange¹⁶ (which should of its very nature be highly sensitive to the band gap) cannot be dominant in those systems. Instead, as we shall show next, the results correlate very well with the predictions based on the notion of superexchange involving filled p shells (valence band) of the anions.

To establish the role of superexchange, we analyze the mutual arrangement of neighboring cations and anions as follows. The tetrahedral radii of Cd and Mn (or Hg and Mn) ions are different.^{15,17} Hence, the tetrahedra formed by both magnetic and nonmagnetic cations surrounding a given anion distort the anion position. One can expect that the superexchange in this case¹⁸⁻²⁰ will be influenced by this distortion. Direct evidence for the distorted configuration of the anion relative to the neighboring Mn^{2+} cations comes from the work of Balzarotti *et al.*,²¹ who have shown that in $\text{Cd}_{1-x}\text{Mn}_x\text{Te}$ the Mn—Te bond length remains almost constant, independent of the Mn content x .

A simple way of representing the distortion of the anion position inside the tetrahedron is through the angle $\tilde{\theta}$ which the anion makes with two neighboring Mn^{2+} ions in a given system, as shown in Fig. 14. One can say that if the cation at the top of a given tetrahedron (i.e., Cd or Hg) is larger than the Mn^{2+} ion, it forces the anion downward, and thus increases the angle $\tilde{\theta}$ with respect to its ideal value of $\tilde{\theta}_0 \approx 109.6^\circ$, whereas if the top cation is of small size, such as Zn, $\tilde{\theta} < 109.6^\circ$. The amount of distortion $\Delta\tilde{\theta}$ will depend on the number of cations of a given type at the corners of the tetrahedron. For $x \leq 0.5$ one can safely say that, if the two bottom cations are Mn^{2+} , then on the average the remaining two will be nonmagnetic. This configuration will be assumed in the analysis

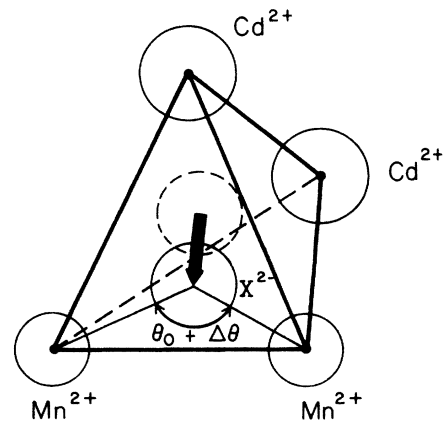


FIG. 14. The distorted position of the anion X^{2-} in the mixed crystal $\text{Cd}_{1-x}\text{Mn}_xX$. The arrow indicates the amount of the distortion with respect to the ideal tetrahedral configuration ($\tilde{\theta}_0 = 109.6^\circ$) in MnX when it is in the structure of the host semiconductor. In $\text{Zn}_{1-x}\text{Mn}_xX$ the distortion will take place in the opposite direction. The angle $\Delta\tilde{\theta}$ determines the corresponding change of the superexchange integral (see the text).

which follows. The discussion for $x > 0.5$ will be given at the end of this section.

It is well known that the value of the superexchange integral depends on the angle which the anion makes with the two neighboring magnetic cations (see, e.g., Ref. 19). Therefore, the change of the angle $\tilde{\theta}$ between one system (e.g., $\text{Cd}_{1-x}\text{Mn}_x\text{Te}$) and another (e.g., $\text{Hg}_{1-x}\text{Mn}_x\text{Te}$) should be reflected in the difference between the values of J_1 for those two cases. The superexchange integral depends explicitly on the angle $\tilde{\theta}$ in the following manner:¹⁸

$$J(\tilde{\theta}) = J(\pi/2)[J(\pi) - J(\pi/2)]\cos^2\tilde{\theta}, \quad (6.1)$$

where $J(\pi/2)$ and $J(\pi)$ are the superexchange integrals for $\tilde{\theta} = 90^\circ$ and 180° , respectively. It is also known that usually¹⁹ $J(\pi/2) \simeq 2J(\pi)$, so that $J(\tilde{\theta})$ decreases as $\tilde{\theta}$ increases with respect to the ideal tetrahedral configuration $\tilde{\theta}_0$.

In order to calculate the amount of distortion $\Delta\tilde{\theta}$ from $\tilde{\theta}_0$, it is reasonable to assume that $\Delta\tilde{\theta}$ should depend on the difference Δa between the cation-cation distances for $x=0$ and 1. That is, the difference between the cation-cation distance of the two binary compounds provides a measure of the distortion $\Delta\tilde{\theta}$ with respect to the ideal tetrahedral configuration of magnetic ions in a hypothetical compound MnX ($X=\text{S}, \text{Se}, \text{or Te}$), which is the limiting case for the semimagnetic semiconductor $A_{1-x}\text{Mn}_x\text{X}$ as $x \rightarrow 1$. These cation-cation distances are 4.484, 4.175, and 3.971 Å for MnTe, MnSe, and MnS, respectively, as shown in Fig. 13. One should emphasize that those distances are the same for both wurtzite and zinc-blende structures, and therefore we do not need to specify the particular type of crystal structure in subsequent discussion.

The relative values of $\Delta a/a_{\text{MnX}}$ are quite small (cf. Fig. 13). Hence we assume that, to a good approximation, $\Delta\tilde{\theta} \simeq \Delta a/a_{\text{MnX}}$. Thus, the change ΔJ of the superexchange integral can be expressed as

$$\Delta J(\tilde{\theta}) = \Delta a/a_{\text{MnX}}[J(\pi/2) - J(\pi)]\sin 2\tilde{\theta}_0, \quad (6.2)$$

where a_{MnX} is the $\text{Mn}^{2+}\text{-Mn}^{2+}$ distance in MnX . Since $\tilde{\theta}_0 = 109.6^\circ > 90^\circ$, the function ΔJ should be a decreasing function of $\Delta a/a$. In Fig. 15 we have plotted the values of J_1 from Table I as a function of the ratio $\Delta a/a$. A linear and decreasing function gives indeed an excellent fit for the tellurides $\text{Cd}_{1-x}\text{Mn}_x\text{Te}$, $\text{Hg}_{1-x}\text{Mn}_x\text{Te}$, and $\text{Zn}_{1-x}\text{Mn}_x\text{Te}$.

On the basis of this agreement one can make the following predictions. Since the selenides are expected to behave in a similar way, one can draw a parallel line which goes through the points for $\text{Hg}_{1-x}\text{Mn}_x\text{Se}$ and $\text{Cd}_{1-x}\text{Mn}_x\text{Se}$. This gives us an expected value of $2J_1/k_B = (32 \pm 1)$ K for $\text{Zn}_{1-x}\text{Mn}_x\text{Se}$. This value has been found very recently by Shapira *et al.*²² to be about 36 K, which is within 10% of our prediction. Furthermore, the values of the exchange integral J_1 for the hypothetical compounds MnSe and MnTe in either the wurtzite or the zinc-blende phases will correspond to the undistorted structure, i.e., $\Delta a = 0$. Figure 15 predicts for these compounds $2J_1/k_B = 28$ and 17 K, respectively.

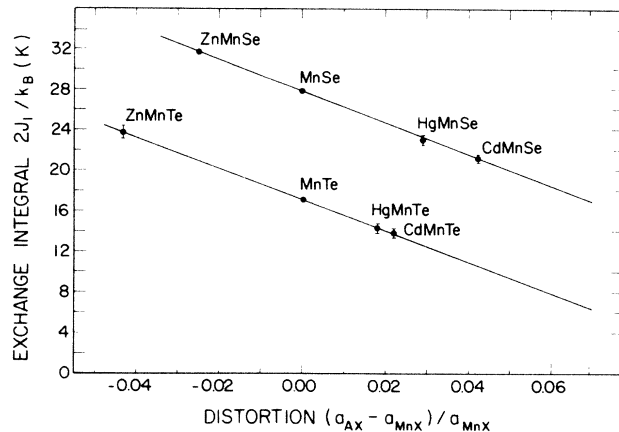


FIG. 15. The exchange integrals $2J_1/k_B$ for selenide and telluride DMS's, specified as a function of the distortion $\Delta a/a$ from the ideal tetrahedron. The lines predict the values of the exchange integrals of the hypothetical magnetic semiconductors MnTe and MnSe, and of $\text{Zn}_{1-x}\text{Mn}_x\text{Se}$, as marked by solid dots (without error bars).

These results can be compared with the recent empirical tight binding method (ETBM) calculations²⁰ for $\text{Cd}_{1-x}\text{Mn}_x\text{Te}$, which yield the value $2J_1/k_B = 24$ K for $x = 0.30$ in this compound. One should mention that in view of the result obtained in Ref. 21, these values should not depend strongly on x , particularly in the region of x substantially lower than 0.5.

Summarizing, one notes a linear and decreasing dependence of J_1 on $\Delta a/a$, as predicted. Furthermore, the values in Fig. 15 for the selenides are higher than those for the tellurides, which corresponds to the circumstance that the tetrahedral radius of Se is smaller than that of Te and hence the Mn-Se distance is smaller than the Mn-Te distance. Since J_1 is consistently stronger in the selenide DMS's than in the corresponding tellurides, these facts constitute a direct indication of the importance of the superexchange mechanism in these systems. It would be interesting to perform the same type of analysis for the sulfides. One should note that the above conclusion, based on correlating the Mn-X distances, does not depend on the concentration x . This is because, as shown recently by Balzarotti *et al.*²¹ with the help of extended x-ray-absorption fine-structure technique, the bond length between two specific constituents in ternary compounds is nearly independent of composition.

Finally, one should comment on the deviation of the Curie-Weiss temperature from a linear dependence on x , seen in Fig. 7 for $\text{Cd}_{1-x}\text{Mn}_x\text{Te}$ and in Fig. 11 for $\text{Zn}_{1-x}\text{Mn}_x\text{Te}$. Namely, for $x \gtrsim 0.5$ the number of undistorted tetrahedrons increases proportionally to x^2 , since this is the probability of having the remaining corners of the tetrahedron occupied by Mn^{2+} ions. Since $\Theta(x)$ already contains a factor of x due to the dilution of Mn^{2+} ions, the resultant dependence of the deviation $\Delta\Theta$ on x is $\Delta\Theta \sim \Theta(x)x^2$, or $\Delta\Theta \sim x^3$, as shown in Fig. 12.

B. Relation between the d - d and p - d exchange integrals

Having demonstrated the importance of superexchange in DMS's, we can now speculate on some relations between d - d and p - d exchange integrals within the superexchange model, which allows us to test the model further. The principal idea of superexchange is based on the notion of the admixture of the p -wave function representing the completely filled anion band to the neighboring $3d^5$ states of Mn^{2+} . The $3d$ electrons are strongly correlated since, as we have shown, Hund's rule is fulfilled, i.e., the spin of the $3d^5$ configuration is close to $\frac{5}{2}$. The narrow $3d$ band is then split into two Hubbard subbands,²³ with both t_{2g} and e_g components half-filled. The width of the respective $3d$ bands is determined mainly by hybridization with the p electrons of the anions, because the direct d - d overlap should be small (owing to the Mn-Mn distances given in Fig. 13).

In order to estimate the amount of the p - d hybridization, we consider the situation depicted schematically in Fig. 16. The perturbed anion wave function p'_σ with spin σ is given by²⁴

$$\begin{aligned} p'_i &= (1+b^2)^{-1/2}(p_i + bd_{A_i}), \\ p'_\uparrow &= (1+b^2)^{-1/2}(p_\uparrow + bd_{B_\uparrow}). \end{aligned} \quad (6.3)$$

In this equation p_σ denotes the unperturbed Wannier function of the p state, and $d_{A,B\sigma}$ are the atomic d -wave functions with spin σ in the positions A and B , whereas b describes the amount of p - d mixing. For simplicity we will not separate the d function into e_g and t_{2g} components. The coefficient b is usually called the covalency factor, which can be written to a first-order approximation as

$$b = \frac{\langle p_\uparrow | H | d_{B_\uparrow} \rangle}{\Delta\epsilon - U_{\text{eff}}} = \frac{\langle p_\uparrow | H | d_{A_\uparrow} \rangle}{\Delta\epsilon - U_{\text{eff}}}, \quad (6.4)$$

where $\Delta\epsilon = \epsilon_p - \epsilon_d$ is the difference between the position of the center of gravity of the p band (i.e., valence band) and the position of the d^5 level, and U_{eff} is the intra-atomic Coulomb repulsion energy between the electrons on the d orbitals, i.e., the energy of the $3d^5 \rightarrow 3d^6$ transition.

Next we will express the d - d transfer (hopping) of an electron induced by the p - d mixing. The contribution to the hopping integral $t_{AB} \equiv \langle d_{A\sigma} | H | d_{B\sigma} \rangle$ describing the motion of the d electron between the two Mn^{2+} ions arises from p - d mixing in the second order. It is estimated to be

$$t_{AB} = b^2(\Delta\epsilon - U_{\text{eff}}). \quad (6.5)$$

The hopping integral, in turn, determines the bare bandwidth of the d states, $W_d = 2z |t_{AB}|x$, where z is the number of nearest neighbors (12 for both the zinc-blende and the wurtzite structures). The value of t_{AB} is needed in order to calculate the superexchange integral J_1 within the Anderson formalism²⁵ (also called the kinetic exchange), given by

$$\frac{2J_1}{k_B} = \frac{2t_{AB}^2}{4S^2k_B U_{\text{eff}}} = b^4 \frac{(U_{\text{eff}} - \Delta\epsilon)^2}{2S^2 U_{\text{eff}} k_B}. \quad (6.6)$$

Furthermore, one should note a very interesting and unique feature inherent in the $A_{1-x}^{\text{II}}\text{Mn}_x\text{X}$ systems. Namely, the virtual $p \leftrightarrow d$ transitions drawn in Fig. 16 as dashed lines will determine the magnitude of the antiferromagnetic coupling of the holes at the top of the valence (p) band with $3d$ spins of Mn. The p - d exchange integral J_{pd} is then

$$J_{pd} \equiv |\beta N_0| = \frac{U_{\text{eff}}(U_{\text{eff}} - |\Delta\epsilon|)^2}{(U_{\text{eff}} - |\Delta\epsilon'|)|\Delta\epsilon'|S} b^2, \quad (6.7)$$

where $\Delta\epsilon'$ is the distance in energy between the position ϵ'_p of the top of the valence band and the position of the $3d^5$ level ϵ_d . This result is similar to that which one gets when calculating the exchange interactions between the magnetic impurities in a nonmagnetic metal with the Wolff model.²⁶ However, the uniqueness of DMS's arises from the circumstance that in the present systems both the d - d (J_1) and p - d (J_{pd}) exchange constants can be determined independently, and with good accuracy.²⁷

The approach presented above predicts correctly the antiferromagnetic character of both the d - d and the p - d interactions, through Eqs. (6.6) and (6.7). However, the exchange interaction between the conduction (s) electrons and the d electrons is ferromagnetic. It appears to take place mainly through direct s - d exchange and therefore should be calculated separately. This is because the covalency factor b_s for the s - d interaction is expected to be smaller than for the p - d interaction, since the d level is located in the p band.^{28,29}

It is very important to know the ratio of the bandwidth W_d of the d band to the magnitude of the intra-atomic interactions, W_d/U_{eff} , since this is the quantity which

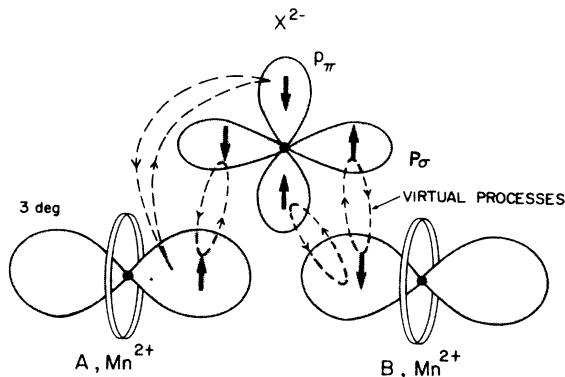


FIG. 16. Schematic representation of the closest Mn^{2+} - X^{2-} - Mn^{2+} configuration for both zinc-blende and wurtzite structures, where X^{2-} is the intervening anion. Only one of the $3d$ e_g orbitals is drawn, whereas both π and σ types of orbitals for p electrons are shown. The arrows specify the spin orientation on a given orbital. The virtual hopping processes lower the energy of the system if the Mn^{2+} spins are mutually antiparallel, and thus lead to the antiferromagnetic exchange of both p - d and d - d types.

determines the nature of the d states in a particular compound. Using the experimentally determined value²⁷ of $J_{pd}=0.88$ eV for $\text{Cd}_{1-x}\text{Mn}_x\text{Te}$ in Eq. (6.7), as well as the approximate position of the $3d^5$ level with respect to the top of the valence p band, $|\Delta\epsilon'| \simeq 3.5$ eV (estimated from the photoemission data^{28,29} for that compound), and assuming the values of unscreened $U_{\text{eff}} \simeq 10-12$ eV and of $\Delta\epsilon \simeq 0$, one gets $b^2 \simeq 0.04$. This, with the aid of Eq. (6.5), gives $W_d \simeq 1$ eV for $x=1$. This result is corroborated by the fact that the same parameters, used in Eq. (6.6), give $2J_1/k_B \simeq 18-26$ K, which is close to the value obtained from ETBM calculations²⁰ for $\text{Cd}_{1-x}\text{Mn}_x\text{Te}$ when we take $U_{\text{eff}}=10$ eV, and also close to that determined from Fig. 15 for MnTe in the zinc-blende structure (17 K) for $U_{\text{eff}}=12$ eV. The small value of b also predicts that the diminution of the value of the atomic spin from $S=\frac{5}{2}$ due to the $p-d$ mixing is small, $\Delta S = b^2 S \simeq 0.1$, which is consistent with our experimental findings. Our value of W_d disagrees with that obtained by Zahorowski and Gilberg,²⁹ who find $W_d \simeq 4.6 \pm 2.7$ eV. We feel, however, that the self-consistency of our result with other microscopic parameters presented above argues in favor of the smaller value of W_d .

Probably the most interesting result which can be inferred from the above estimate is the fact that

$$W_d/U_{\text{eff}} \sim 0.1 \ll 1.$$

This indicates that the $3d$ band is quite narrow, and therefore the splitting due to the correlations among the d electrons leads to the Hubbard subband structure.²³ Thus, the narrow d band in DMS's contains the same principal features as found in the classical Mott insulators MnO , MnS , MnSe , and MnTe .³⁰ In DMS's, the band is, of

course, narrowed additionally by the dilution of magnetic ions.

VII. CONCLUDING REMARKS

We conclude with two remarks. The analysis of the exchange interaction presented in this paper gives only one effective integral J_1 , associated with nearest-neighbor interactions. It is now being realized that the exchange integral J_2 for next-nearest neighbors, while much smaller than J_1 , is nonetheless important in determining the thermodynamic properties in the dilute limit $x \lesssim 0.2$ at low temperatures,³¹ and that it may affect the nature of the antiferromagnetic ordering³² for $x \geq 0.5$. Hence, it would be desirable to extend the present analysis to lower temperatures, in order to determine J_2 explicitly.

Furthermore, an interesting question arises whether the high-temperature properties can be related to the onset of spin-glass behavior at low temperatures. In the next part of this series we plan to show that for the wide-gap semiconductors the spin-glass freezing temperature $T_f(x)$ is proportional to the Curie-Weiss temperature $\Theta(x)$ obtained here. This shows again the importance of the high-temperature regime in revealing the close relationship between the interactions which govern the paramagnetic and the spin-glass behavior in these diluted magnetic systems.

ACKNOWLEDGMENTS

The authors wish to thank D. Yoder-Short and U. Debska for the use of Fig. 13. Support by National Science Foundation (Materials Research Laboratories Program) Grant No. DMR-83-16988 is gratefully acknowledged.

*Present address.

¹For a review of fundamental properties, see R. R. Galazka, in *Proceedings of the 14th International Conference on the Physics of Semiconductors, Edinburgh, 1978*, edited by B. L. H. Wilson (IOP, Bristol, 1979), p. 133; and J. K. Furdyna, *J. Appl. Phys.* **53**, 7637 (1982).

²U. Sondermann, *J. Magn. Magn. Mater.* **2**, 216 (1976); U. Sondermann and E. Vogt, *Physica* **86-88B**, 418 (1977).

³H. Savage, J. J. Rhyne, R. Holm, J. R. Cullen, C. E. Carroll, and E. P. Wohlforth, *Phys. Status Solidi B* **58**, 685 (1973).

⁴S. B. Oseroff, *Phys. Rev. B* **25**, 6584 (1982).

⁵ $\text{Hg}_{1-x}\text{Mn}_x\text{Te}$ data is taken from S. Nagata, R. Galazka, D. P. Mullin, G. D. Khattak, J. K. Furdyna, and P. H. Keesom, *Phys. Rev. B* **22**, 3331 (1980).

⁶ $\text{Zn}_{1-x}\text{Mn}_x\text{Te}$ data is taken from S. P. McAlister, J. K. Furdyna, and W. Giriat, *Phys. Rev. B* **29**, 1310 (1984).

⁷A. Mycielski and J. Mycielski, *J. Phys. Soc. Jpn.* **49**, Suppl. A, 807 (1980); T. Wojtowicz and A. Mycielski, *Physica* **117-118B**, 476 (1983).

⁸T. Dietl and J. Spałek, *Phys. Rev. Lett.* **48**, 355 (1982); *Phys. Rev.* **B28**, 1548 (1983); D. Heiman, P. A. Wolff, and J. Warnock, *Phys. Rev. B* **27**, 4848 (1983).

⁹See, e.g., the tables published in W. Marshall and S. W. Lovesey, in *Theory of Thermal Neutron Scattering* (Pergamon, Oxford, 1971).

¹⁰Z. Obuszko, Patent No. 95 119, Poland (unpublished).

¹¹The value for HgSe was measured; χ_d for CdSe and CdTe were taken from V. I. Ivanov-Omskii, B. T. Kolomiets, V. M. Melnik, and V. K. Ogorodnikov, *Fiz. Tverd. Tela (Leningrad)* **11**, 2563 (1969) [*Sov. Phys.—Solid State* **11**, 2067 (1970)].

¹²R. R. Galazka, in *Proceedings of the 14th International Conference on the Physics of Semiconductors, Edinburgh, 1978*, Ref. 1.

¹³One should be careful in ascribing any serious meaning to the Curie-Weiss law for the Mn concentrations for which the temperature $|\Theta(x)|$ is comparable to (and especially when it exceeds) the highest temperature $T=300$ K at which the measurement of χ was performed. This is one of the reasons why the data for low $x \leq 0.3$ are the most important for our purposes. For a recent discussion of the limitations of the Curie-Weiss law in a more general context, see A. S. Arrott, *Phys. Rev. B* **31**, 2851 (1985).

¹⁴R. E. Kremer and J. K. Furdyna, *Phys. Rev. B* **31**, 1 (1985).

¹⁵D. Yoder-Short, U. Debska, and J. K. Furdyna, *J. Appl. Phys.* **58**, 4058 (1985).

¹⁶C. Lewiner, J. A. Gaj, and G. Bastard, *J. Phys. (Paris)* **41**, C5-289 (1980); G. Bastard and C. Lewiner, *Phys. Rev. B* **20**, 4256 (1979); J. Ginter, J. Kossut, and L. Swierkowski, *Phys. Status Solidi B* **96**, 735 (1979); L. Liu, *Solid State Commun.* **35**, 187 (1980).

- ¹⁷J. A. Van Vechten and J. C. Phillips, *Phys. Rev. B* **2**, 2160 (1970).
- ¹⁸See, e.g. C. Boekema, F. Van der Waude, and G. A. Sawatzky, *Int. J. Magn.* **3**, 341 (1972).
- ¹⁹J. Owen and J. H. M. Thornley, *Rep. Prog. Phys.* **29**, 675 (1966).
- ²⁰B. E. Larson, K. C. Hass, H. Ehrenreich, and A. E. Carlsson, *Solid State Commun.* **56**, 347 (1985).
- ²¹A. Balzarotti, A. Kisiel, N. Motta, M. Zimnal-Starnawska, M. T. Czyżyk, and M. Podgórnny, *Phys. Rev. B* **31**, 7526 (1985).
- ²²Y. Shapira, S. Foner, D. H. Ridgley, K. Dwight, and A. Wold, *Phys. Rev. B* **30**, 4021 (1984).
- ²³J. Hubbard, *Proc. R. Soc. (London) Ser. A* **281**, 401 (1964); a discussion in analytic terms for a system of resonant d states with a Lorentzian density of states is given in M. Acquarone, D. K. Ray, and J. Spałek, *J. Phys. C* **15**, 959 (1982).
- ²⁴G. A. Sawatzky, W. Geerstma, and C. Haas, *J. Magn. Magn. Mater.* **3**, 37 (1976).
- ²⁵P. W. Anderson, *Phys. Rev.* **115**, 1 (1959); also in *Solid State Physics*, edited by F. Seitz and D. Turnbull (Academic, New York, 1963), Vol. 14, pp. 99-214.
- ²⁶J. Spałek, A. M. Oleś, and K. A. Chao, *Phys. Rev. B* **18**, 3748 (1978); *Phys. Status Solidi B* **87**, 628 (1978). The same type of interaction has been considered for DMS's within the context of the Anderson model for a magnetic impurity by A. K. Bhattacharjee, G. Fishman, and B. Coqblin, *Physica* **117-188B**, 449 (1983).
- ²⁷For a review of the values of J_{pd} determined by optical methods, see J. A. Gaj, *J. Phys. Soc. Jpn. Suppl. A* **49**, 797 (1980).
- ²⁸C. Webb, M. Kamińska, M. Lichtensteiger, and J. Lagowski, *Solid State Commun.* **40**, 609 (1981).
- ²⁹W. Zahorowski and E. Gilberg, *Solid State Commun.* **52**, 921 (1984).
- ³⁰J. W. Allen, G. Lucovsky, and J. C. Mikkelsen, Jr., *Solid State Commun.* **24**, 367 (1977).
- ³¹R. R. Galazka, S. Nagata, and P. H. Keesom, *Phys. Rev. B* **22**, 3344 (1980); S. Nagata, R. Galazka, D. P. Mullin, G. D. Khattak, J. K. Furdyna, and P. H. Keesom, *Phys. Rev. B* **22**, 3331 (1980). The properties of DMS's at low temperatures are described in terms of an effective temperature $T_0 \sim 1.2$ K for $x=0.05$. This is a phenomenological procedure and was introduced by J. A. Gaj, R. Planel, and G. Fishman, *Solid State Commun.* **29**, 435 (1979). See also W. Dobrowolski, M. von Ortenberg, A. M. Sandauer, R. R. Galazka, A. Mycielski, and R. Pauthenet, in *Physics of Narrow Gap Semiconductors*, Vol 152 of *Lecture Notes in Physics*, edited by E. Gornik, H. Heinrich, and L. Palmetshofer (Springer-Verlag, Berlin, 1982).
- ³²T. Giebultowicz (private communication).

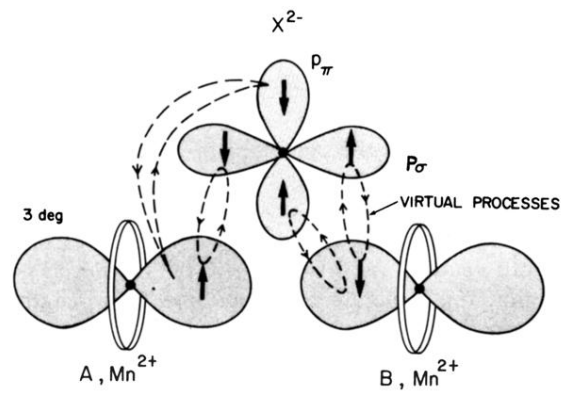


FIG. 16. Schematic representation of the closest Mn^{2+} - X^{2-} - Mn^{2+} configuration for both zinc-blende and wurtzite structures, where X^{2-} is the intervening anion. Only one of the $3d$ e_g orbitals is drawn, whereas both π and σ types of orbitals for p electrons are shown. The arrows specify the spin orientation on a given orbital. The virtual hopping processes lower the energy of the system if the Mn^{2+} spins are mutually antiparallel, and thus lead to the antiferromagnetic exchange of both p - d and d - d types.